Synthetic Metals 273 (2021) 116693

Contents lists available at ScienceDirect

Synthetic Metals

journal homepage: www.elsevier.com/locate/synmet

Review

Interfacial polymerization for controllable fabrication of nanostructured conducting polymers and their composites

Nan Gao [a,1], Jiarui Yu [a,2], Shuai Chen [a,b,c,*,3], Xing Xin [c,4], Ling Zang [b,**,5]

[a] Flexible Electronics Innovation Institute and School of Pharmacy, Jiangxi Science & Technology Normal University, Nanchang, Jiangxi 330013, China
[b] Nano Institute of Utah and Department of Materials Science and Engineering, University of Utah, Salt Lake City, UT 84112, United States
[c] Jiangxi Engineering Laboratory of Waterborne Coatings, Jiangxi Science & Technology Normal University, Nanchang, Jiangxi 330013, China

ARTICLE INFO

Keywords:
Conducting polymer
Nanostructure
Interfacial polymerization
Oxidative polymerization
Organic electronics

ABSTRACT

Nanostructured conducting polymers (NCPs) have been extensively studied in various organic electronic fields because of their unique, excellent structural, mechanical, electric and photoelectric properties at the nanoscale. The sizes and morphologies of NCPs, which are highly dependent on the original molecular structure and synthesis optimization, play critical roles in the applications involving NCP materials. As a promising strategy among the chemical oxidative polymerization methods, interfacial polymerization (IP) has been used in creation of abundant NCP materials through facilely controlled interfacial oxidative reactions. Here, we present a special review on the research progress of tunable IP involving different interfaces (liquid-liquid, liquid-solid, vapor-solid and vapor-liquid), wherein the precursor monomers can be positioned in either of the two phases. Such highly tunable interfacial fabrication has been proven an effective method for making NCPs and their composites both with controllable structure and properties. The nanostructured materials fabricated therefrom have found broad, increasing applications in supercapacitor, sensor, corrosion protection and other fields as discussed as well in this review. Also given at the end of this review are a summary and prospective overview about the current research issues and future development. It is expected that this review will provide systematic assistance and inspire new ideas for the development of interfacial processing technique in the field of nanostructured polymers.

1. Introduction

Conducting polymers (CPs) containing conjugated backbones have been of great interest to both fundamental and applied research since the discovery of highly conducting polyacetylene in 1976, due to their unique and intrinsically tunable conductivity and flexibility, as well as inherent optical, electrochemical and photoelectronic properties [1]. Till now, multitudinous CPs especially polyaniline (PANI), polypyrrole (PPy), polythiophene (PTh), poly(3,4-ethylenedioxythiophene) (PEDOT), and their derivatives, have been widely studied and applied in organic electronic fields related to energy, environment, biology, health and safety (Fig. 1) [1,2]. However, the development of the properties of CPs has not been completely commensurate with those of their metallic and inorganic semiconductor counterparts. Consequently, CPs have constantly been hybridized with other materials to overcome their inherent limitations and improve properties essential to the electronic or optoelectronic applications [3]. On the other hand, by confining the dimensions of bulk CPs into nanoscale, nanostructured conducting polymers (NCPs) and their composites with diverse sizes and morphologies such as nanoparticles, nanorods, nanofibers, nanotubes, and so on, possess large surface area, optimal electrical conductivity, improved carrier mobility, superior electrochemical activity and good

* Corresponding author at: Flexible Electronics Innovation Institute and School of Pharmacy, Jiangxi Science & Technology Normal University, Nanchang, Jiangxi 330013, China.
** Corresponding author.
E-mail addresses: shuaichen@jxstnu.edu.cn (S. Chen), lzang@eng.utah.edu (L. Zang).
[1] ORCID: 0000-0001-5071-3453
[2] ORCID: 0000-0002-9215-663X
[3] ORCID: 0000-0001-8566-601X
[4] ORCID: 0000-0002-5122-7104
[5] ORCID: 0000-0002-4299-0992

https://doi.org/10.1016/j.synthmet.2020.116693
Received 28 October 2020; Received in revised form 12 December 2020; Accepted 25 December 2020

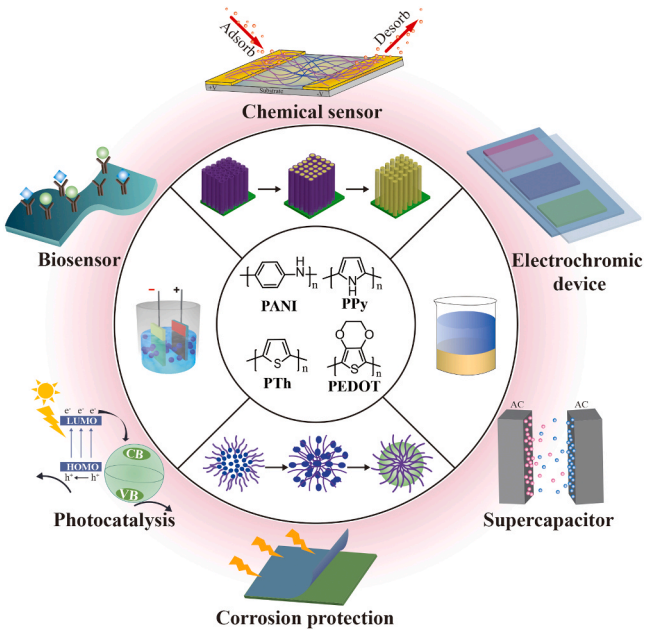

Fig. 1. An overview of synthesis methods and applications of NCPs.

mechanical properties, *etc*., which combined make them ideal candidate for application in biological, optoelectronic, and energy-related fields as shown in Fig. 1 [4,5].

Chemical oxidation or electrochemical polymerization are the two most widely used techniques in synthesis of NCPs. While the electrochemical approaches require special workstations [6], oxidative polymerization methodologies based on hard template, soft template or even template-free (Fig. 1) (e.g., interfacial polymerization, seeding approach) have been developed, and these facile fabrication techniques have riven to be conducive to size and morphology control of NCPs in diverse applications [7]. Among them, the hard template method requires physical templates such as track-etched polycarbonate (PC), polyester (PE) and anodic aluminum oxide (AAO) membranes and other solid porous materials (e.g., zeolites, *etc*.) as molds to control the polymerization processes and nanostructure in terms of morphology and sizes, and additional process is required to remove the template, which may result in the deformation of the as-prepared NCPs. On the contrary, soft template method relies on relatively simple and inexpensive fabrication process including micro-/mini-emulsion polymerization, reversed-microemulsion, layer-by-layer self-assembly and block copolymer mediated synthesis, *etc*., though the weak control intrinsic to the soft template over the uniformity of morphology still remains a challenge. In general, template method is technically limited in use of template and the necessary post-synthesis treatment. On the other hand, the electrochemical polymerization and physical methods such as electro-spinning and mechanical stretching can also produce NCPs, but these methods require special instrumentation and energy-consuming operation [6,7]. Standing beyond the methods above, as mentioned in our recent review [7], a method called “interfacial polymerization (IP)” initially explored by Huang et al. [8] can be used for template-free synthesis, which can produce pure and uniform NCPs with small dimensions in bulk quantities. In general, IP was performed in an aqueous/organic biphasic system, in which monomer of CP is dissolved in an organic solvent and the oxidant is dissolved in an aqueous solution. The aqueous/organic interface formed is stable, allowing for controllable synthesis of NCPs through localized polymerization reaction upon the contact between monomer and oxidant. In addition to such initial IP reaction at liquid-liquid interface, others including liquid-solid, vapor-solid and vapor-liquid interfaces have also been studied and developed for IP process, which enable the use of gas, liquid or solid reactants, thus much broadening the scope of NCP synthesis as described in detail in Section 2.

IP reaction is generally considered to be a template-free approach, that is, high concentration monomer molecules and oxidative doped anions react immediately at the interface, producing monomer-anion (or oligomer-anion) aggregates, which lead to formation of polymers. Nonetheless, to further control the morphology of NCPs by tuning reaction components in the biphasic system, some researchers have tried to add some additives acting as templates into the reaction systems [9–11]. This may be the reason why IP is sometimes also described as a soft-template method [12]. It is worthy to note that the IP process is distinct from another nanostructure fabrication method called interfacial self-assembly [13–15], which is based on mass transfer control of building block molecules at the interface between a good and poor solvent. Therein the self-assembly is driven by a combination of optimal intermolecular interactions including hydrogen bonds, Van der Waals forces, π-π stacking interaction, metal coordination and other weak dispersive forces, whereas no covalent chemical reactions or polymerizations are involved. Taking a series of n-type organic semiconductor molecules, perylene-3,4,9,10-tetracarboxylic diimides (PTCDIs), as the classical building blocks, our group has successfully fabricated a broad range of nanofibers with uniform one-dimensional (1D) morphology and sizes, for which the π-π stacking between the high planar skeletons of PTCDIs plays critical role in concert with the interfacial mass transfer control [13–15].

In recent years, several relevant reviews have been published by Yunze Long [12], Michiel J.T. Raaijmakers [16], Thanh-Hai Le [17], Yongyang Song [18], as well as us [7]. However, these reviews cover only partially the topics about synthesis strategies, morphological characteristics or applications of NCPs (involving IP of different monomers). It still remains imperative to provide a deep review with more specific focus on how to regulate the structures and morphologies of NCPs via tunable IP processes, for which the precursor monomer can be positioned optionally in one of the two phases between liquid and liquid, liquid and solid, vapor and liquid, and vapor and solid. Herein we present a comprehensive overview of the recent research progress of tunable IP at various interfaces for controllable fabrication of NCPs and the composites thereof. Also covered in this review are the broad applications of NCPs in supercapacitor, sensor, corrosion protection and other related fields. Finally, a summary and prospective overview about current technical challenges and future development of IP synthesis of NCPs are provided, with a hope to inspire more research interest and effort into this exciting, promising field.

2. Tunable interfacial polymerization for fabrication of NCPs

According to the interface where the polymerization reaction of monomer and oxidant occurs, IP fabrication of NCPs can be classified into four types as shown in Fig. 2, liquid-liquid interface with monomer in one the two phases (Lm-L), liquid-solid interface with monomer in either phase (Lm-S, L-Sm), vapor-solid interface with monomer in the vapor phase (Vm-S), and vapor-liquid interface with monomer in the vapor phase (Vm-L), where “m” represents monomer dissolved in one phase around the interface. These immiscible biphasic systems enable the mild initiation and propagation of the oxidation reaction with fewer nucleation sites essentially being restricted at the interface, compared to the rapid, disorder and bulk-phase reaction employed in traditional single-phase synthesis. In this section, we will discuss in detail the monomer structures, interface design and the control of reaction conditions, which all have significant effect on the nanostructure formation and morphology of NCPs (nanofiber, nanotube, nanoparticle, *etc*.). A variety of polymers such as PANI, PPy, PTh, PEDOT, *etc*. have been involved in the research and will be discussed in this section. Summarized in Table 1 are some typical examples of NCPs and their nanocomposites synthesized in different IP reaction systems, which demonstrate varying morphologies and interesting applications.

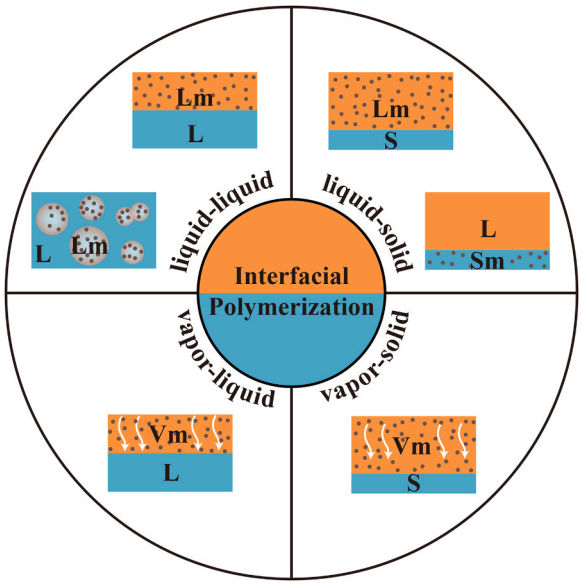

Fig. 2. Typical interface systems used in IP: liquid-liquid (Lm-L), liquid-solid (Lm-S, L-Sm) vapor-liquid (Vm-L) and vapor-solid (Vm-S), wherein "m" is the monomer dissolved in one of the two phases around the interface.

Specially, we carefully distinguish the IP reactions from other polymerization reactions at substrate surfaces, wherein the monomer and oxidant reactants are usually premixed such as in-situ oxidative polymerization [1].

2.1. Liquid-liquid (Lm-L) interface

As the most commonly studied interface for IP synthesis, Lm-L allows for the polymer reaction to take place at the interface of two immiscible liquids, usually an aqueous or organic phase containing oxidant and an organic phase with monomer dissolved. NCPs formed at the interface will diffuse away from the interface and get populated in the aqueous or organic phase (driven by solubility), thus leaving a fresh interface behind for new polymerization until all the reactants are consumed. As a result, secondary growth of NCPs is suppressed and the initially formed nanostructures can be maintained upon dispersing in the liquid phase. In comparison, in the conventional synthesis, the freshly formed NCPs remain surrounded by monomers and oxidants, which may facilitate the formation of nucleation centers, and thus further precipitation, eventually growing into irregularly shaped granular particles [8]. To some extent, such IP process is reminiscent of the bisolvent interfacial self-assembly of PTCDI molecules into 1D nanostructures particularly nanofibers, whereas the later often adopts two miscible but density different organic solvents [14]. Overall, the structure and morphology of NCPs from IP are highly relied on the concerted control of selection of organic solvents and oxidants, type and concentration of monomers, reaction time and conditions like temperature, *etc*. Some other factors like additives or composite ingredients also play significant role in the IP synthesis.

Up to now, a great variety of organic solvents have been used to construct Lm-L interface including diethyl ether, CH_2Cl_2, $CHCl_3$, CCl_4, hexane, benzene, toluene, and among others. In general, less toxic solvents heavier than water are preferred for IP synthesis for safety reason since supernatant water atop can help to seal the organic vapor within the reaction vessel [8]. Stirring is often used in IP synthesis to speed up the reaction, as it helps create more Lm-L interface (i.e., larger interfacial area) for the polymerization. It was found that a slower stirring rate was favorable for obtaining higher doping level, but the morphology uniformity of the nanofibers formed was not as good as that obtained at the faster stirring rate [19]. It has been also reported that the type of organic phase has little effect on the morphology and nanostructure of PANI prepared through IP [8,20,21], though this remains in debate. The solvent miscibility will influence the monomer diffusivity and solubility in the opposite phase. When the solubility of monomer in the opposite phase is low, the resulting polymer structure tends to be denser or more agglomerated, unlike nanofibers formed by the rapid diffusion into water. Zhang et al. [22] creatively introduced a kind of ionic liquid, [BMIM]PF_6 as a "buffering zone" between the aqueous and organic phases. The high viscosity of the ionic liquid layer regulates the diffusion rate of aniline from CCl_4 to the aqueous phase, which influences the subsequent polymerization process and favors for the enhancement of molecular order. The synthesized coral-like PANI possesses much better electrochemical performance and desirable electronic conductivity due to its unique structure and large specific surface area. More specifically, for polymerization of thiophene, both the two phases of IP have to be organic solvent because almost no PTh can be obtained if using organic/aqueous interface. PTh nanoparticles are commonly obtained in hexane (thiophene)-acetonitrile (CH_3CN) ($FeCl_3$) IP system [23].

NCPs such as PTh [23], PPy [24], polyindoles [25,26], polycarbazoles [27], and PEDOT [28] whose monomers are insoluble in water have been realized by IP strategy in Lm-L systems. Nanostructured PANI has also been successfully synthesized via IP into various morphologies such as nanofiber [8], nanoneedle [29] and nanotube [30]. In view of its good solubility in common organic solvents and low cost, aniline (monomer of PANI) has been the most popular monomer used in IP synthesis of NCPs. IP of aniline requires additional protonic acid dopants to work together with the oxidants, which are the key to maintain the electrically conductive feature of PANI (Indeed, PANI remains as one of the most investigated and promising CPs for wide commercial applications) [1,17]. For a generic example, the IP reaction of aniline into PANI nanofibers at the water/CH_2Cl_2 interface can be driven by a strong oxidant like ammonium peroxydisulfate (APS) dissolved in a protonic solution like 1 M hydrochloric (HCl) acid [8]. Although various dopant acids, inorganic types (HCl, sulfuric acid (H_2SO_4), nitric acid (HNO_3), phosphoric acid (H_3PO_4), perchloric acid ($HClO_4$), *etc*.) or organic types (ethanoic acid, methanoic acid, tartaric acid, camphor sulfonic acid, methyl sulfonic acid, ethyl sulfonic acid, 4-toluene sulfonic acid, *etc*.) can be used in IP of aniline, their counter ion types and acidity in various reaction media are found to have significant effect on the formed nanostructures of PANI and their properties through controlling the proportions between neutral aniline molecules/anilinium cations and deprotonated/protonated states [31]. Li et al. [32] found that nanofibril, nanogranular and hollow ball-like morphology of PANI can be formed by using acids HCl, H_2SO_4 and HNO_3, respectively. The morphology difference seems to be consistent with relative oxidation capability of HCl < H_2SO_4 < HNO_3 acid. Under the condition of HCl, the PANI nanofibers formed can rapidly diffuse into the aqueous phase due to their hydrophilic nature, thus avoiding overgrowth. In comparison, under the condition of HNO_3, the amphiphilic charged HNO_3-aniline salt could self-assemble into sticklike micelles as soft templates and aniline oligomers with high concentration assembled into hollow nanostructure. In the case of H_2SO_4, PANI exhibited nanogranular morphology, because H_2SO_4 has a larger size of counterpart ion. The doping of PANI chains accompanied with the counterparts near backbones can result in PANI with relatively short chains and low molecular weights when protons were attached onto amine or imine groups in molecule chains. Besides, the average diameter of PANI with the same nanofiber morphology was also found to increase with acidic strength in water-CH_2Cl_2 IP system, which can be tuned from 30 nm using HCl to 120 nm using $HClO_4$ acid [8]. In another example, on account of the strong interfacial hydrogen bonding action between a special acid $H_4SiW_{12}O_{40}$ and water molecules, aligned belt nanostructures of PANI have been fabricated in water-CH_2Cl_2, water-toluene and water-diethyl ether IP systems [33]. The water molecule layers located in the interface have an ordered array, and strong hydrogen bonding between water molecules and $H_4SiW_{12}O_{40}$ leads to $H_4SiW_{12}O_{40}$

Table 1
Morphology and applications of selected NCPs synthesized in different IP reaction systems.

NCPs	Morphology	Interface	Reaction system	Oxidant	Application	Ref.
PANI	nanofiber	Lm-L	CH_2Cl_2-H_2O	APS (dopant: various acid)	–	[8, 20]
PANI-PSS	nanofiber	Lm-L	CCl_4-H_2O	APS (dopant: PSS)	–	[9]
PANI	nanoneedle, nanofiber	Lm-L	$CHCl_3$-H_2O	APS, H_2O_2 (dopant: HCl)	–	[10]
	slightly elongated structure	Lm-L	$CHCl_3$-H_2O	APS, H_2O_2 (dopant: HCl) (additive: DTAB)		
	spherical, nanofiber	Lm-L	$CHCl_3$-H_2O	APS, H_2O_2 (dopant: HCl) (additive: SDS)		
PANI	nanoneedle, hollow microsphere, nanowire	Lm-L	$CHCl_3$-H_2O	APS (dopant: HCl) (additive: CTAB)	–	[11]
PANI	nanofiber	Lm-L	xylene-H_2O	APS (dopant: HCl)	–	[19]
PANI	nanofiber	Lm-L	$CHCl_3$-H_2O	APS (dopant: HCl) (additive: IPA)	supercapacitor	[21]
PANI	coral-like	Lm-Lb[a]-L	CCl_4-[BMIM]PF_6-H_2O	APS	supercapacitor	[22]
	nanosheet	Lm-Lb-L	CCl_4-[EMIM]BF_4-H_2O	APS		
PTh	microparticle	Lm-L	hexane-CH_3CN/CH_3NO_2	$FeCl_3$	–	[23]
PPy/PDMS	film	Lm-L	hexane-H_2O	$FeCl_2$ and $FeCl_3$	gas separation	[24]
polyindole	nanoparticle	Lm-L	$CHCl_3$-H_2O	APS	–	[25]
polyindole	nanorod	Lm-L	CH_2Cl_2-H_2O	APS (dopant: H_2SO_4)	–	[26]
polycarbazole	macroporous honeycomb	Lm-L	CH_2Cl_2-H_2O	APS (dopant: HCl) (additive: Tween20)	–	[27]
	connected hollow sphere	Lm-L	CH_2Cl_2-H_2O	APS (dopant: HCl) (additive: CTAB)		
	smaller hollow sphere	Lm-L	CH_2Cl_2-H_2O	APS (dopant: HCl) (additive: SDS)		
PEDOT	nanoneedle	Lm-L	CH_2Cl_2-H_2O	$FeCl_3$	–	[28]
PANI	nanoneedle	Lm-L	CH_2Cl_2-H_2O	$FeCl_3$	–	[29]
PPy	nanoneedle	Lm-L	CH_2Cl_2-H_2O	$FeCl_3$		
PANI	nanofiber	Lm-L	toluene-H_2O	APS (additive: $MgCO_3$)	–	[30]
	nanotube	Lm-L	toluene-H_2O	APS (additive: $CaCO_3$)		
PANI	nanofiber	Lm-L	$CHCl_3$-H_2O	$FeCl_2$ and CHP[b] (dopant: HCl)	supercapacitor	[32]
	granular	Lm-L	$CHCl_3$-H_2O	$FeCl_2$ and CHP (dopant: H_2SO_4)		
	hollow ball-like	Lm-L	$CHCl_3$-H_2O	$FeCl_2$ and CHP (dopant: HNO_3)		
PANI	aligned belt	Lm-L	CH_2Cl_2-H_2O	$FeCl_3$ (dopant: $H_4SiW_{12}O_{40}$)	–	[33]
PANI	petal-like	Lm-L	CCl_4-H_2O	APS and $K_2Cr_2O_7$ (dopant: HCl)	supercapacitor	[35]
PANI	spongey nanospherical	Lm-L	hexane-CH_3CN	MTPPS (dopant: p-TSA)	supercapacitor	[38]
PEDOT	nanocapsule, mesocellular foam	Lm-L	cyclohexane-H_2O	CAN (additive: DeTAB)	supercapacitor	[39]
PANI	nanofiber	Lm-L	CH_2Cl_2-H_2O	APS (additive: CeO_2)	–	[40]
PANI	nanofiber	Lm-L	$CHCl_3$-H_2O	APS (dopant: HCl) (additive: CH_3OH or C_2H_5OH)	supercapacitor	[41]
PANI	nanofiber	Lm-L	$CHCl_3$-H_2O	APS (dopant: HCl) (additive: acetone)	supercapacitor	[42]
PPy/PANI	nanoparticle	Lm-L	CCl_4-H_2O	APS (dopant: HCl) (additive: CTAB)	H_2 gas sensor	[43]
PANI/PTh	nanoparticle	Lm-L	$CHCl_3$-H_2O	APS (dopant: H_2SO_4)	supercapacitor	[44]
PANI/PDMA	nanoparticle	Lm-L	$CHCl_3$-H_2O	APS (dopant: HCl)	–	[45]
CB/PPy	hollow nanosphere	Lm-L	toluene-H_2O	APS	supercapacitor	[46]
graphene/PANI/MnO_2	nanofiber	Lm-L	$CHCl_3$-H_2O	APS and $KMnO_4$ (dopant: H_2SO_4)	supercapacitor	[47]
Au/PANI	nanofiber	Lm-L	toluene-H_2O	APS (dopant: H_2SO_4)	–	[48]
MnO_2/PANI	nanorod	Lm-L	toluene-H_2O	MnO_2 (dopant: H_2SO_4)	photocatalytic	[49]
poly(ionic liquid)s@PANI	core-shell microsphere	L-Sm	C_2H_5OH and H_2O-poly(ionic liquid) microsphere	APS	electro-responsive electrorheological	[52]
PANI/cotton	smooth fiber	L-Sm	H_2O-cotton	APS	–	[53]
PEDOT	nanofilm	Lm-S	cyclohexane-PET sheet	$Fe(OTs)_3$	–	[54]
PEDOT	film	Lm-S	$CHCl_3$-PI film	H_2O_2 and $FeCl_3$	–	[55]
PCL/PANI	porous film	Lm-S	H_2O-PCL-BPO film	PCL-BPO film (dopant: HCl)	–	[56]
PEDOT	nanofiber	Vm-S	EDOT-rusted steel	rusted steel (dopant: HCl)	supercapacitor	[57]
PEDOT/CNT	3D scaffold	Vm-S	EDOT-cylindrical shaped template	$FeCl_3$	electroactive tissues	[58]
PPy/CNT	3D scaffold	Vm-S	pyrrole-cylindrical shaped template	$FeCl_3$	electroactive tissues	[59]
PPy/PANI	film	Vm-L	pyrrole and aniline-H_2O	$FeCl_3$	Cr(VI) adsorption	[61]
PANI	irregular shape and size	Vm-L	aniline-H_2O	APS (dopant: HCl)	–	[62]
PANI	nanofiber	Lm-L	toluene-H_2O	APS (dopant: HCl)	NO_2 gas sensor	[65]
GCs/PANI	3D hollow	L-Sm	H_2O-GCs	APS (dopant: HCl)	NH_3 gas sensor	[66]
PANI	nanofiber	Lm-L	$CHCl_3$-H_2O	APS (dopant: HCl)	corrosion protection	[71]
PANI	nanotube	Lm-L	xylene-H_2O	APS (dopant: DPA and HCl)	corrosion protection	[72]

[a] Ionic liquid as "buffering zone" between organic and aqueous phases.
[b] Cumene hydroperoxide.

aligning along the water molecule layers of the interface, while providing protons to the aniline (Fig. 3a). These actions result in an ordered array of aniline or polymer chains at the interface, forming PANI in belt-like nanostructure (Fig. 3b). Compared with HCl-doped PANI nanofibers (Fig. 3c) formed in the same water-diethyl ether IP system, the PANI nanobelts doped with $H_4SiW_{12}O_{40}$ possess a more ordered structure as indicated by the diffraction peak in XRD spectrum (Fig. 3d), and the higher ordered structure is consistent with the higher electrical conductivity observed (Fig. 3e).

In addition to the molecular dopants, just as evidenced in the famous case of PEDOT:PSS [34], sulfonated polystyrene (PSS, acidic polymer with pKa smaller than that of aniline, 4.63) can also be used as a proton source to provide the necessary counterions to charged PANI, and can also help maintain the water solubility of the final PANI-PSS nanofiber complex [9]. The resulting water-casting processable, transparent, conducting film showed morphology of nanofibers (40–50 nm in diameter) imbedded in low emissive polystyrene chains; the nanofibers reveal twisted surface, unlike the neat nanofibers prepared under the presence of camphorsulfonic acid (CSA).

For successful IP reaction in Lm-L bisolvent system, water-soluble oxidants such as iron(III) salts [24], APS [8], hydrogen peroxide (H_2O_2) [10], potassium dichromate [35] are usually required. The component and concentration are the two critical factors that affect the IP of monomers forming CPs. For example, in water-hexane IP system, addition of $FeCl_2$ can slow down the reaction between pyrrole and $FeCl_3$, leading to formation of denser structured PPy nanofilm [24]. Composite oxidants have also been studied, and found to be capable of adjusting the nanostructures of PANI. As reported by Zeng et al., [35] nanostructures of PANI can be controlled and tuned from nanofibers synthesized with APS as oxidant to nano-petal-like morphology in water-CCl_4 IP system by using a composite oxidant APS/$K_2Cr_2O_7$. Because the oxidability of APS/$K_2Cr_2O_7$ is much higher than that of single oxidant APS, which accelerated the polymerization of aniline, forming a large number of oligomers at the initial stage of IP which then aggregated into nano-petal-like PANI. When low concentrations of oxidant and monomer are used together, the IP reaction will be significantly slowed down, and the crystallization time at the interface can be further extended so as to increase the degree of crystallization, yielding higher crystalline NCPs. For a specific case when 0.1 mg/mL of $FeCl_3$ and 1 mg/mL of monomer were used in a water-CH_2Cl_2 IP system, single-crystalline nanoneedles of PANI (size 63 nm × 12 nm), PPy (size 70 nm × 20 nm) were formed, while single-crystalline nanoneedles of PEDOT (size 50 nm × 15 nm) were formed under 1 mg/mL $FeCl_3$ and 1 mg/mL monomer [28,29]. After attacked by the oxidant, IP reaction occurred along the vertical direction of the interface and the oriented polymers were aligned during the slow IP reaction to form elongated rice-like crystals.

Another point worthy to be noted about control of IP is the molar ratio between the oxidant and the monomer. For example, the [APS]/[aniline] ratio is usually controlled at 1/4 in order to synthesize uniform PANI nanofibers. With the increase of ratio, the fibrillar morphology became more and more aggregation, and almost disappeared at ratio of 1/1. This is because the concentration of the initially generated PANI nanofibers at interface increased at high [APS]/[aniline] ratio, leading to rapid aggregation of PANI before diffusing into aqueous phase [36,37]. Though not common, some oxidants soluble in organic solvents can also be used in IP. By using methyltriphenylphosphonium peroxodisulfate (MTPPS) as the oxidant, spongy PANI nanospheres were formed at the interface of hexane (containing aniline)-CH_3CN (containing MTPPS) [38].

Additives such as surfactants in aqueous or organic phase have significant influence on the aggregation of aniline oligomers. In the traditional homogeneous reaction system with surfactant, micelles formed by monomer and surfactant were regarded as templates supporting the formation of nanostructures [10]. Differently for IP reaction, micelles composed of monomer, oxidant and surfactant might be formed at the reaction interface between aqueous and organic solvent. The spherical micelles formed in the IP might be regarded as templates enabling formation of hollow microspheres through a self-assembly process at the interface. Broad range of morphologies of NCPs could be obtained by using different surfactants at varying concentrations. Dallas et al. [10] investigated the effects of surfactant type (dodecyltrimethylammonium bromide (DTAB) and sodium dodecylsulfate(SDS)) on the IP synthesis of PANI in water-$CHCl_3$ system, from which slightly elongated

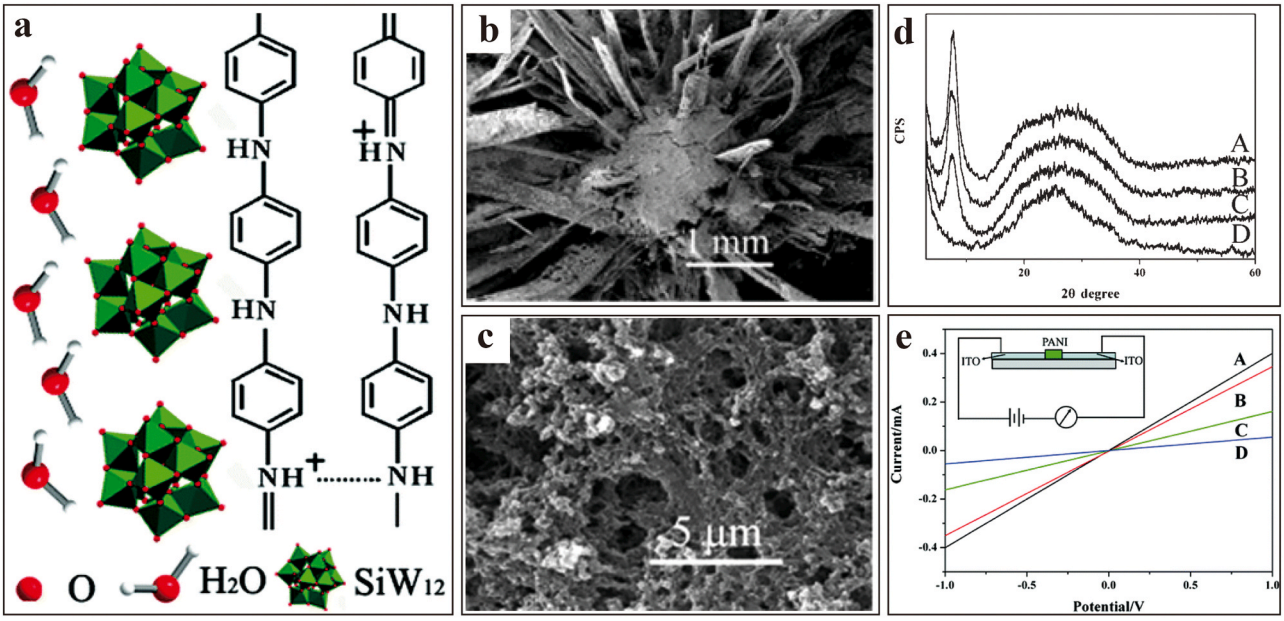

Fig. 3. (a) Scheme for the formation mechanism of PANI belts at Lm-L interface. SEM images of (b) aligned PANI belts synthesized by water-diethyl ether IP approach using $H_4SiW_{12}O_{40}$ as doping acid and (c) PANI fibers obtained by water-diethyl ether IP approach using HCl as doping acid. (d) XRD patterns and (e) I-V characteristic of a conductivity testing of PANI by using different doping acid and organic solvents: (A) $H_4SiW_{12}O_{40}$ (methylene chloride), (B) $H_4SiW_{12}O_{40}$ (toluene), (C) $H_4SiW_{12}O_{40}$ (diethyl ether), and (D) HCl (diethyl ether). (inset: schematic of the ITO-PANI-ITO device).
Reprinted with permission from Ref. [33]. Copyright 2011 American Chemical Society.

nanostructure and nanospherical shape were obtained, respectively. In another example, morphology change of nanostructured PANI from nanoneedles or nanowires with a network architecture to hollow microspheres was observed in water-$CHCl_3$ IP system simply by changing the surfactant concentration of cetyltrimethylammonium bromide (CTAB) [11]. With increasing CTAB concentration, the morphology of micelles changed from spherical to linear, which might be regarded as templates supporting the formation of networked nanowires. Similarly, PEDOT nanocapsules and mesocellular foams were fabricated and formation of the morphology was strongly dependent on the concentration of decyltrimethylammonium bromide (DeTAB) [39]. In the study, a variable amount of DeTAB was dissolved in distilled water forming micelles, and cerium ammonium nitrate (CAN) was added to the micelle solution as oxidant. The micelles are able to capture the oxidant due to electrostatic interactions between CAN and the surfactant molecules, and this allows oxidant to exist at the micelle/water interface. The micelle solution was then introduced dropwise into cyclohexane solution containing monomer EDOT which comes into contact with oxidant at the micelle interface (Fig. 4a). By changing the concentration of DeTAB, the morphology of PEDOT formed was changed from nanocapsules to mesocellular foams (Fig. 4b–d) [39].

He et al. [30,40] synthesized PANI nanotubes and nanofibers by IP in a solids-stabilized oil-water emulsion, in which nanoparticles ($MgCO_3$, $CaCO_3$, CeO_2) were used as emulsifiers. When these nanoparticles were mixed with water and organic solvent $CHCl_2$ or toluene under stirring, solids-stabilized emulsion (often referred to as Pickering emulsion) could be obtained even though there were no surfactants used. The organic solution was dispersed in the water phase and nanoparticles were situated at the organic/water interface. As a consequence, aniline in the droplets of the emulsion would diffuse to the interface and get polymerized under the oxidation of APS in the water phase.

Additionally, some intermolecular interactions between polymers chains and solvent molecules play roles to certain extent in tuning the morphology and nanostructures of NCPs. It is reported that when small alcohol molecules like methanol and ethanol were introduced into aqueous phase, the strong intermolecular hydrogen bonding between PANI chains and alcohol molecules could significantly suppress the growth and migration of PANI nanofibers. As a result, PANI nanofibers with increasing length-diameter ratio and relatively higher orientation of polymer chains could be obtained [41]. Similarly, Zhao et al. [42] observed that addition of acetone molecules could also suppress the IP process as well, thus leading to formation of PANI nanofibers with smaller diameter and higher orientation of polymer chains.

Lm-L interface is not only the most commonly used IP system for the synthesis of pure NCPs as mentioned above, but also has been developed for synthesizing nanostructured copolymers such as PPy/PANI [43], PANI/PTh [44] and PANI/Poly(2-methoxyaniline) (PANI/PDMA) [45], for which the morphologies obtained are usually in the form of nanoparticles (Fig. 5). For example, PANI/PTh copolymer synthesized in water-$CHCl_3$ IP system showed nanoparticle morphology in the size of 40–60 nm [44]. In the synthesis, both the aniline and thiophene monomers were dissolved in the $CHCl_3$ phase. Some other copolymers like PANI/PDMA have also been studied for the IP synthesis as reported by Abdelwahab et al. [45], and the molar ratio of two monomers was found to affect significantly the morphology of NCPs synthesized. Upon changing the molar ratio of aniline and 2-methoxyaniline from 1/4 or 4/1 to 1/1 in $CHCl_3$, the morphology of the copolymer PANI/PDMA synthesized changed from nanoparticle (4–10 nm) to narrow nanofiber (4–8 nm in diameter).

NCPs are often combined with other nanomaterials including carbon nanomaterials [46,47], metal [48] and metal oxide [49] nanoparticles, *etc*. to enhance the properties towards particular applications. Besides, as nanomaterials are added into the liquid phase where IP reactions occurred, they are also served as templates for the synthesis of composites with special morphologies. Monomers are polymerized in the presence of these nanomaterials which can be added to the aqueous or organic phase and maintain homogeneous dispersion under ultrasound treatment or stirring during the IP synthesis. For example,

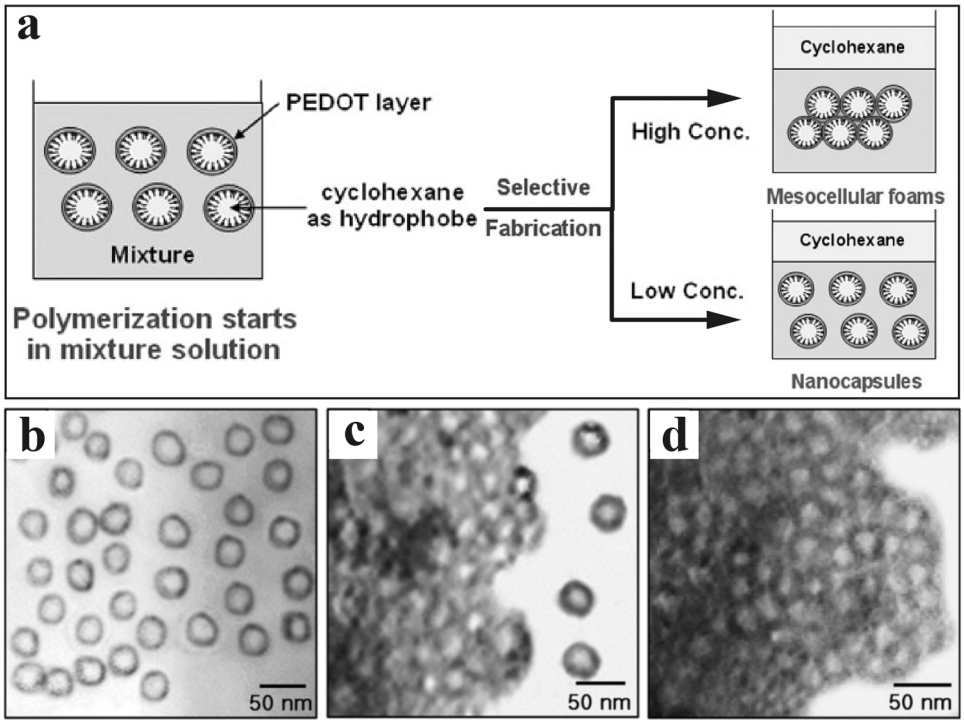

Fig. 4. (a) The overall procedure for the selective fabrication of PEDOT nanocapsules and mesocellular foams via Lm-L IP process involving cyclohexane solution containing monomer and DeTAB water micelles. TEM images of PEDOT (b) nanocapsules, (c) mixture of nanocapsules and mesocellular foams and (d) mesocellular foams prepared with 0.15 M, 0.20 M and 0.30 M DeTAB, respectively.
Reprinted with permission from Ref. [39]. Copyright 2006 WILEY-VCH.

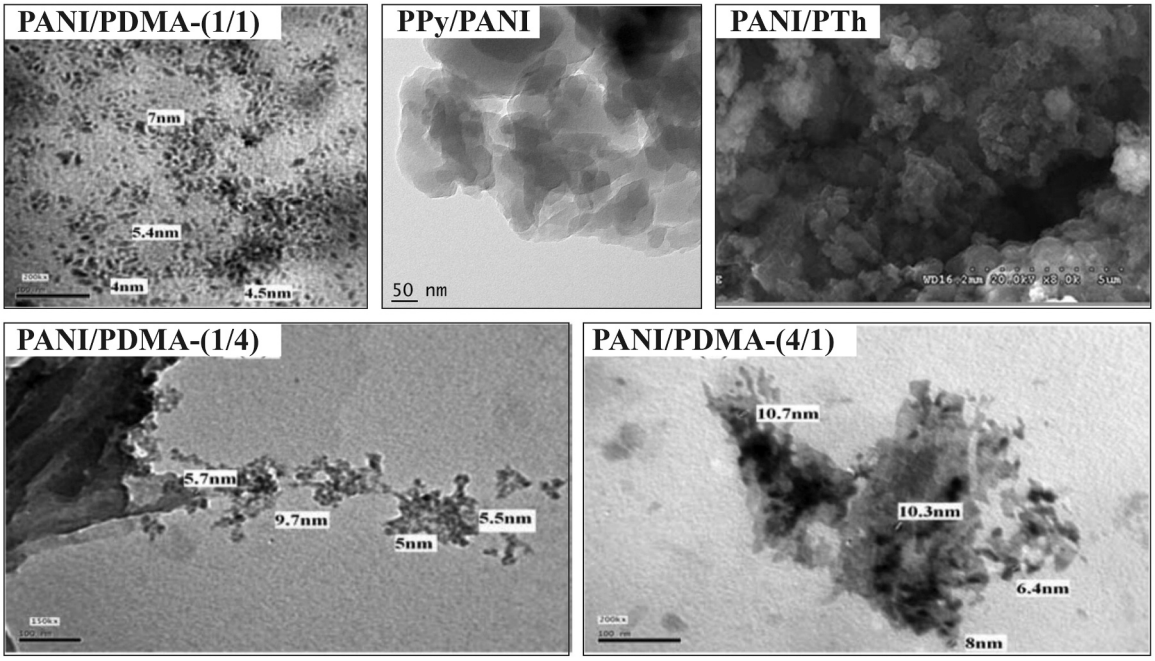

Fig. 5. TEM image of PPy/PANI nanoparticles. FESEM image of PANI/PTh nanoparticles. TEM images of PANI/PDMA nanofibers and nanoparticles with the molar ratio of aniline and 2-methoxyaniline of 1/1, 1/4 and 4/1.
TEM image of PPy/PANI nanoparticles: Reprinted with permission from Ref. [43]. Copyright 2020 Elsevier B.V. FESEM image of PANI/PTh nanoparticles: Reprinted with permission from Ref. [44]. Copyright 2015 Wiley Periodicals, Inc. TEM images of PANI/PDMA nanofibers and nanoparticles: Reprinted with permission from Ref. [45]. Copyright 2013 Taylor & Francis Group, LLC.

PANI-modified MnO_2 composite nanorods were fabricated via IP of aniline in the presence of MnO_2 nanorods at water/toluene interface [49]. Clearly, appropriate additives like the nanomaterials mentioned above could result in significant effect on the control of morphology of NCPs and their composites fabricated through IP; further research along this direction by using different nanomaterials or nanostructures as templates should be taken into account.

2.2. Liquid-solid (Lm-S, L-Sm) interface

The IP reaction at Lm-S or L-Sm interface can be considered as a heterogeneous reaction system, which is distinct from the Lm-L cases described above. Typically, monomers (or oxidants) are coated onto a solid substrate (template), which will then be brought into contact with a liquid phase where dissolved the oxidant (or monomer) to initiate the IP reaction at the solid-liquid interface [50]. Apparently, in such a case the IP reaction is limited (highly localized) to the solid surface as one of the reactants (monomer or oxidant) is preabsorbed on the surface. The surface supported reaction helps produce polymers in nanostructures that match the structural pattern of the substrate, thus providing a promising way to control the morphology of nanostructured polymers and their composites. Commonly used solid-phase substrates include both rigid and flexible films, as well as some polymer templates like poly (etheretherketone) (PEEK) [1,51].

Between the two types of liquid-solid interfaces, L-Sm interface is relatively uncommonly used in IP, but it is easy for synthesizing composite micro-/nano-materials due to the strong surface adhesion of monomers on the solid substrate or template [52,53]. For L-Sm IP, variable factors play critical roles in controlling the NCPs structures and morphologies, including solid phase materials and their proportion with monomers, the type and proportion of monomers and oxidants, and other experimental conditions like temperature, solvent and concentrations. For example, taking advantage of the hydrophilic character of aniline and poly(ionic liquid)s, Zheng et al. [52] synthesized core-shell poly(ionic liquid)s@PANI microspheres, in which poly(ionic liquid)s microspheres surface provided the reaction interface between absorbed aniline and later-contacted oxidant APS. The thickness of PANI shell can be adjusted by controlling the dosage of aniline, however, when the mass ratio of aniline to poly(ionic liquid)s was higher than 3/7, individual granular PANI appeared. This is because the poly(ionic liquid)s could absorb enough aniline and only small amount of remaining aniline were polymerized in liquid phase.

Compared to L-Sm IP, Lm-S approach (sometimes called liquid phase deposition polymerization [50]) has gained much more attention because it based on stable substrate precast with oxidant, which is practically convenient (and provide wide options) for reacting with different monomers dissolved in a solution (the liquid phase). But to avoid dissolution of the oxidant from surface (especially during the polymerization process), the liquid phase containing monomer should be considered seriously. Since Fe^{3+} salts are the most widely used oxidants for polymerization in CPs fields, and the salts are usually soluble well in water and CH_3CN but not in other normal organic solvents, Li et al. studied the Lm-S IP synthesis of PEDOT nanofilms using Iron(III) p-toluene sulfonate ($Fe(OTs)_3$) [54] or $FeCl_3$ [55] as the oxidant supported on poly (ethylenephthalate) (PET) or polyimide (PI) film, and EDOT as monomer dissolved in cyclohexane or $CHCl_3$. Despite carefully controlling the low content of oxidants on the substrates, there are still traces of oxidant inevitably falling into liquid phase upon immersing substrate into the solution. Nonetheless, it is believed that the trace amount of oxidized oligomers formed in the solution can hardly affect the interfacial formation of polymer film. Much promisingly, they found that using double oxidants of H_2O_2 and $FeCl_3$ and hydrolyzed PI film as substrate was a good choice for IP [55]. A hydrolyzed PI film was immersed first in H_2O_2 solution, then in $FeCl_3$ solution and finally in $CHCl_3$ solution containing EDOT·H_2O_2 would transform carboxylic groups on hydrolyzed PI film to peroxyacid groups, which in turn worked as secondary oxidant together with $FeCl_3$ to promote the polymerization of EDOT on the surface. Other similar Lm-S IP methods using much ingenious oxidant substrates to obtain interesting NCPs were also reported. Male et al. [56] used honeycomb-patterned poly

(ε-carprolactone)-benzoyl peroxide (PCL/BPO) film as oxidizing substrate to realize IP synthesis of flexible and porous PCL/PANI films by contacting the oxidant film with aqueous HCl solution of aniline (Fig. 6a–e). Only nanoscale layer of PANI was formed on the PCL film surface because the oxidant BPO was available only at the film/solution interface, i.e., after certain period of polymerization covering the surface oxidant species, no oxidant is available at the interface to react with the monomer in solution phase. Such surface patterned IP approach is quite useful for developing flexible conductive devices in organic electronics.

2.3. Vapor-solid (Vm-S) interface

For oxidative IP reactions occurring at Vm-S interface, the monomer serves as the vapor phase and the solid phase is usually a substrate containing oxidant, and the whole reaction is held in a sealed reactor that is kept at a constant high temperature or pumped to induce negative pressure to accelerate the evaporation of monomers. Both pure NCPs and their composites have been successfully synthesized with the Vm-S IP methods [57–59]. Formation of high-quality NCPs at Vm-S interface extremely depends on the controlling vapor state, chamber humidity, oxidant formula and reaction conditions. On one hand, it is a challenging task to maintain the homogeneity of monomer vapors in large vacuum chamber. On the other hand, it is very sensitive to humidity in the chamber because high humidity will stimulate the hydration and crystallization of oxidants like Fe^{3+} salts, likely leading to pinholes in the final film by continued cross-linking of NCPs. Also, reaction conditions like temperature could affect significantly the vapor phase state and polymerization rate.

Diao et al. [57] used a rusted steel as oxidant to obtain freestanding PEDOT film with high packing density of nanofibers with a core-shell $FeCl_2$-PEDOT architecture when EDOT/chlorobenzene vapor and HCl vapor made contact with the solid-state rust coating in a sealed reactor at 150 °C (Fig. 7a). 37% HCl was selected to reduce the hydration of Fe^{3+} liberated from bulk rust (FeOOH, $FeSO_4$) by reacting with the HCl vapor, which promoted the vertical growth of PEDOT-coated FeOOH nanofibers. As the reaction continues, Fe^{3+} in FeOOH scaffolds was reduced to Fe^{2+} forming the $FeCl_2$ core (Fig. 7b and c). The importance of the choice and use of oxidants has also been demonstrated by Prato et al., as they prepared three-dimensional (3D) conductive porous PEDOT/carbon nanotube (CNT) scaffolds [58] as well as PPy/CNT scaffolds [59] based on Vm-S IP between EDOT or pyrrole vapor and blended sucrose-CNT-$FeCl_3$ template. In addition to controlling the polymerization time (overnight) and temperature (140 °C), a small amount of strong oxidant (20 mg $FeCl_3$) was found imperative for ensuring that enough polymers can be produced to hold the entire 3D structure, whereas larger quantities of oxidant present would hinder the polymerization because of high humidity from the hydrated oxidant [60].

2.4. Vapor-liquid (Vm-L) interface

With the oxidant existing in the liquid state, the monomer vapor can contact the solution surface to generate the polymerization reaction at the Vm-L interface, just as shown in Fig. 8a [61], which is reminiscent of the vapor-transfer induced molecular self-assembly technique previously developed from our lab [14]. Aqueous solutions of APS or Fe (III)-based oxidant have been used as liquid phase to react with the vapor of highly volatile monomers (e.g., aniline, pyrrole, *etc.*). The vapor can usually be generated by evaporation from a beaker containing the corresponding monomer held in a vacuum desiccator. Pure NCPs [62] or nanostructured copolymers [61] can be formed at these Vm-L interfaces, though they subsequently transformed into film morphology since the initially generated NCPs aggregates still rest on the solution surfaces until the whole reactions stopped. However, due to the constant stirring during the reaction, nanoscale PANI synthesized by this method showed irregular shape, size (the length and diameter of PANI ranging from 50 to 400 nm and 20–100 nm, respectively) and surface, exhibited lower conductivity (due to a less ordered structure with lower crystallinity and crystallite size). On the other hand, the PANI materials thus synthesized showed higher hydrophilicity and higher solubility (lower molecular weight), which may be due to the easier contact between the monomer and oxidant in the vapor phase leading to the growth of higher number of polymer chains with lower length than that of the solution or dispersion state [62].

Fig. 8 shows a representative example for synthesis of copolymer PPy/PANI at Vm-L interface, wherein mixture vapor of two monomers pyrrole and aniline is in contact with the aqueous solution of $FeCl_3$. Film of PPy/PANI (Fig. 8b) has been prepared and displayed a high density of pore-like features with irregular shape and various diameters [61]. The observed porosity is due to the evaporation and diffusion of water vapor through the film, particularly at lower concentration of $FeCl_3$ (Fig. 8c). With the increase of $FeCl_3$ concentration, the pore-on-film structure was no longer observed (Fig. 8d). On the other side, the partial pressure of each monomer in vapor phase should be considered. Since the vapor pressure of pyrrole (8.288 mmHg at 25 °C) is much higher than that of aniline (0.465 mmHg at 25 °C), the PPy film would be formed at the initial stage of IP and acts as polymerization sites supporting the

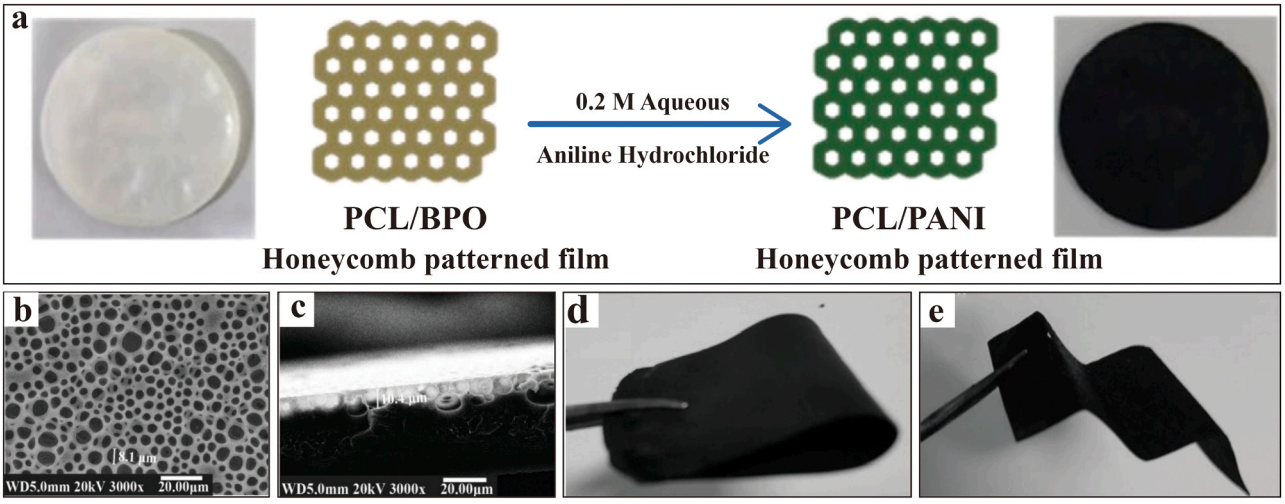

Fig. 6. (a) Schematic representation of the Lm-S IP synthesis of PANI-functionalized-polycaprolactone (PCL) film. (b) Surface and (c) cross-section SEM images of PCL/PANI film. The photos of (d) single and (e) multi-folded PCL/PANI films.
Reprinted with permission from Ref. [56]. Copyright 2016 Elsevier. B.V.

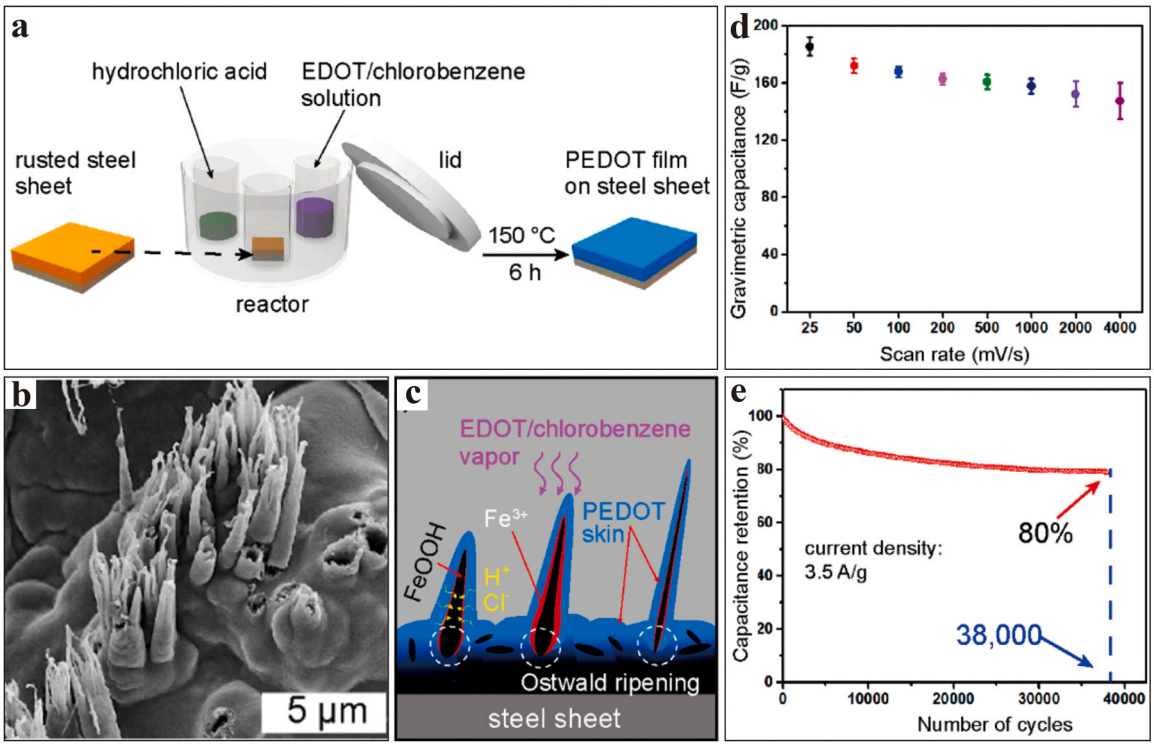

Fig. 7. (a) Schematic illustration of rust-based Vm-S IP in a sealed vessel. (b) 1D core-shell FeOOH-PEDOT microfibers piercing out of the PEDOT film skin, and (c) the schematic mechanism about their growth under Ostwald ripening FeOOH nuclei. (d) The high rate capability retaining gravimetric capacitance at fast scan rates and (e) 80% of original capacitance retained after 38,000 cycles of the two-electrode PEDOT symmetric supercapacitor.
Reprinted with permission from Ref. [57]. Copyright 2019 American Chemical Society.

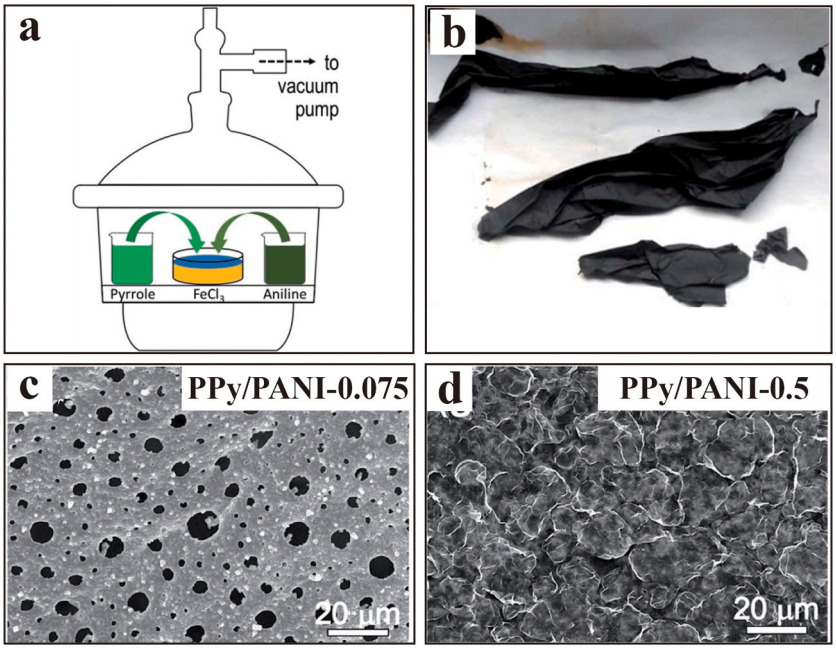

Fig. 8. (a) Schematic illustration of Vm-L IP synthesis of PPy/PANI composite films. (b) Free-standing PPy/PANI composite films. Top-view SEM images of PPy/PANI composite films synthesized with (c) 0.075 M $FeCl_3$ and (d) 0.5 M $FeCl_3$.
Reprinted with permission from Ref. [61]. Copyright 2019 Royal Society of Chemistry.

subsequent polymerization and growth of PANI.

3. Applications of NCPs fabricated by interfacial polymerization

As discussed in previous sections, NCPs and their composites synthesized by IP have been extensively studied and explored for potential applications because of the combination of superiority on large surface area, high electrical conductivity, mechanical flexibility, facile production, easy nano-structuring and low cost. These features make NCPs ideal candidate for development into various electronic devices

and applications, such as supercapacitors, sensors, corrosion protection and among others. In this section, we will elaborate more of these specific applications, with the aim to better understand the structure-property-function relationship, which in turn is very much correlated with the controlled IP and growth of NCPs under varying reaction conditions as described above in previous sections.

3.1. Supercapacitors

Supercapacitors have gained enormous attention due to their unique features like high power, long cycle life and environment-friendly nature. CPs have been extensively studied for applications in supercapacitors due to the remarkable pseudocapacitance behavior originating from the multiple oxidation states of CPs. Since the short diffusion path and high surface area are the two key factors in determining the device power density, NCPs have received remarkable consideration for potential development as supercapacitors [63].

By virtue of great interfacial tunability, IP can be adjusted through various ways mentioned in Section 2, so as to increase crystallinity, regular nanostructure and surface morphology of NCPs there synthesized, which in turn can improve their capacitance performances. In contrast to other nanostructures, nanofiber morphology with a larger length to diameter ratio and higher orientation of polymer chains could provide shorter ion diffusion path, enhanced electroactivity, and increased electrode/electrolyte contact area. By introducing ethanol into aqueous phase of water-$CHCl_3$ reaction system, Jin et al. [41] synthesized uniform PANI nanofibers with larger length-diameter ratio, which exhibited specific capacitance of 489 F g^{-1} at a current density of 1 A g^{-1} and retained 65.4% after 500 cycles. Previously in 2006, PEDOT nanocapsules and mesocellular foams synthesized at water/cyclohexane interface were reported exhibiting rectangular shaped current voltage curves with a steep increase in the current over a potential range of 0.0–0.2 V, which led to a specific capacitance of about 155 and 170 F g^{-1}, respectively [39]. These observed high capacitance values were due to their unique structures and larger specific surface area compared to pristine PEDOT nanoparticles. More recently, film electrode of PEDOT nanofibers synthesized at the Vm-S interface gave a capacitance of 181 F g^{-1} at a current density of 3.5 A g^{-1} and retained 80% of the original data after 38,000 cycles, mainly benefiting from the high packing density in the film of high-aspect-ratio core-shell nanofibers (Fig. 7d and e) [57].

Nevertheless, for electrodes fabricated from pure NCPs there are still some challenges on the aspects of energy density and cycling stability in long term charge-discharge processes. Thus, composites of NCPs containing other active materials like metal oxides or carbon materials have been developed with the hope to synergize the advantageous structure and performance features between them to achieve much higher capacitance and better cycling stability [63]. Transition metal oxide nanoparticles were chosen because of their large surface area, short conduction lengths and inherent electrochemical pseudocapacitive properties, while carbon nanomaterials (carbon black, CNT, graphene, *etc*.) were chosen because of their high accessible surface area, good conductivity and charge transfer channels. As a typical example, Li et al. [47] proposed and synthesized graphene/PANI/MnO_2 hybrids by Lm-L IP, in which graphene was employed as an excellent substrate to host the active polymer and PANI nanofibers as ideal charge transfer and storage carrier. Monomer aniline was mixed with graphene in $CHCl_3$ and polymerized at water/$CHCl_3$ interface by a binary oxidants of potassium permanganate and APS. Although the electrical conductivity of MnO_2 (generated from the oxidation) was inferior to that of PANI, it can act as new nucleation center over terminate growing PANI chains, leading to further chain growth and finally much ordered PANI nanofibers. The hybrids of graphene/PANI/MnO_2 thus fabricated contain electrical double layer capacitance of graphene and pseudo capacitance of PANII and MnO_2, which demonstrated significantly enhanced specific capacitance of 800.1 F g^{-1} at 0.4 A g^{-1}, and remaining 71% of the initial capacitance after 800 cycles, much higher than that of pure PANI nanofibers obtained at water (APS)/$CHCl_3$ (aniline) interface.

3.2. Sensors

Electrical conductivity of NCPs changes drastically upon chemical or electrochemical doping, and such modulation can be developed into sensors taking advantages of the flexibility, ease and low cost of large area processing intrinsic to polymer materials. Holding this great promise, NCPs have drawn increasingly interest in fundamental and applied research in recent years. In addition to the sensitive dependence of conductivity of NCPs on chemical doping (absorption), the sensitivity of NCP based sensors also benefits from the high surface area and small sizes of NCPs, which help facilitate the fast diffusion of analyte molecules onto their surface. Thus, NCPs could be directly developed into chemiresistive sensors to detect a wide range of oxidizing or reducing chemical analytes, especially chemical vapors like alcohols, ethers, ammonia (NH_3), organic volatile amines, nitro explosives, NO_x, H_2, H_2S, SO_2, CO, and among others [64].

In general, just like most of the chemiresistive sensors involving single sensing component (material), sensors made of pure NCPs also often suffer from low sensitivity and poor selectivity, but these can be improved by IP fabrication of high-quality and structurally controlled NCPs. It has been proven that PANI nanofibers with controlled size distributions synthesized at the water/toluene interface could have the gas-phase doping/dedoping time decreased in comparison to the common PANI, owing to the high surface area and small size (30–80 nm) of PANI nanofibers [65]. If complexed with other nanocomponents, like metal or metal oxide nanoparticles, carbon nanomaterials, insulating polymers, the sensing performance of PANI nanomaterials would be further improved. For example, 3D hollow quasi-graphite capsule/PANI (GCs/PANI) hierarchical hybrids (Fig. 9a–e) were constructed by decorating protonated PANI on the surface of GCs [66]. Different amounts of GCs (1, 3, 9 mg) were separately dispersed in water providing the reaction interface between absorbed aniline and later-contacted oxidant APS in HCl solution, which produced different hybrid materials labeled as GC/PANI-1, GC/PANI-3, GC/PANI-9. The rigidly ordered architectures obtained ensure these hybrids with relatively larger interface, which in turn is conducive to surface adsorption of analyte molecules and increased sensing response due to charge transfer. As shown in Fig. 9b, the GCs/PANI-3 hybrid is highly sensitive (with a response ratio of 1.30) toward 10 ppm NH_3 gas with short response and recovery times of 34 and 42 s, respectively. The GCs/PANI-3 material also demonstrates a good selectivity, repeatability, and long-term stability, which are attributed to the synergistic effect of the composite of GCs and PANI. Indeed, the control of interfacial charge transfer is believed to be critical to tune the sensor performance of chemiresistive materials. Recently, we published a systematic review on the p-p/p-n/n-n heterojunction nanofibers (fabricated from various composited of metal oxides, carbon nanomaterials and NCPs, *etc*.) and their applications in gas-phase chemical detection, with specific focus on the structural arrangement of nanofibril heterojunctions so as to tune the interfacial charge transfer kinetics, which in turn leads to adjustment and optimization of the sensing performances [67].

NCPs have also attracted intensive interest in the development of biosensors owing to their excellent biocompatibility and strong immobilization of biomolecules, as well as rapid and efficient electron transfer interactions with biomolecules [7]. The flexibility and biocompatibility of NCPs have also made them highly active in the field of bioelectronics [68]. For example, many researchers have developed NCPs-based electronic skins or wearable sensors that can sense pressure, touch, emotional change, temperature, sweat, breath chemicals, *etc*. These emerging applications open new broader research scenarios for NCPs and the associated IP synthesis, wherein the interfacial improvement demands a lot more research regarding both materials design and engineering.

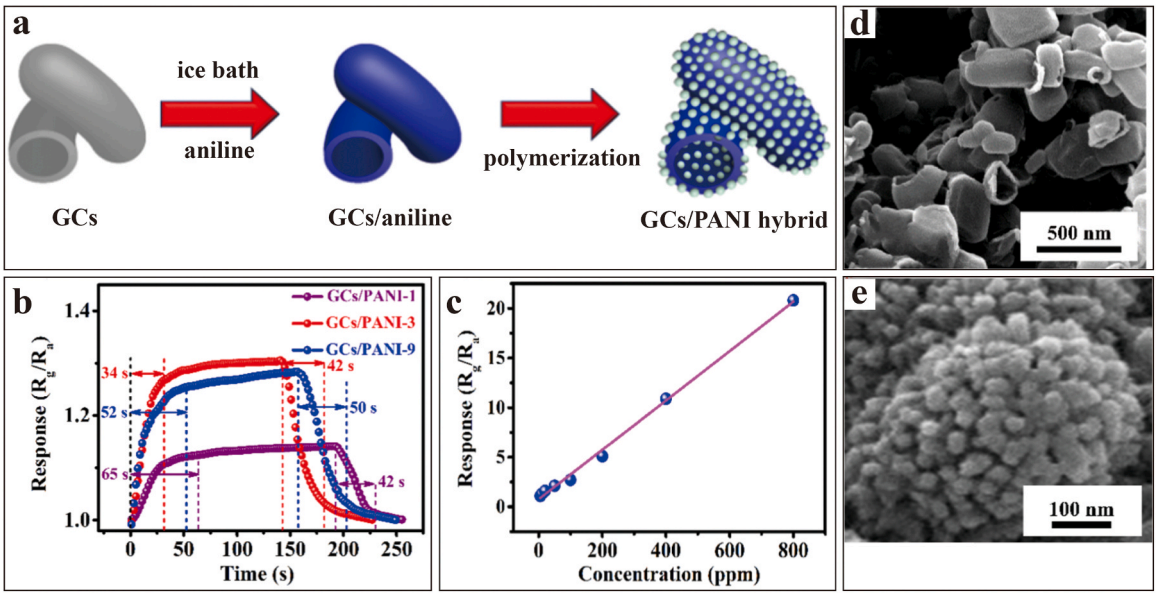

Fig. 9. (a) Schematic illustration of fabrication of the GCs/PANI hybrid composites. (b) Dynamic response-recovery curves of the GCs/PANI-1, GCs/PANI-3, and GCs/PANI-9 based sensors toward 10 ppm NH_3. (c) A calibration plot of the response of the GCs/PANI-3 sensor versus the concentration of NH_3 in the range of 5–800 ppm. SEM images of the (d) pure GCs and (e) GCs/PANI-3 hybrid.
Reprinted with permission from Ref. [66]. Copyright 2019 American Chemical Society.

3.3. Corrosion protection

Metal corrosion has caused huge economic losses and serious safety risks, making the research of green and environmental benign functional anti-corrosion coatings quite attractive. In order to achieve long-term and anodic protection, Deberry et al. [69] first reported the application of CPs in the field of corrosion protection. It is believed that CPs promote the formation of passivating layer at the interface between metal and CPs, thus slowing down the corrosion. Since then, it has been found that more CPs like PANI, PPy and others can also provide corrosion protection for highly oxidizable metals such as iron, aluminum and zinc. CPs have thereby become a fresh hotspot in anti-corrosion coating research, taking advantage of the diversified structure, unique doping mechanism and high environmental stability intrinsic to CPs [70]. Besides polymer chain itself, morphology and type of dopants also affect the anti-corrosion properties. However, in order to sustain the anti-corrosion capability, CPs are often blended with other polymers (e.g., polyvinyl butyral and polyvinyl chloride) that possess good mechanical characteristics and can provide backup protection after the CPs are eventually consumed from the redox reactions.

NCPs, particularly those with highly controlled structure and morphology fabricated from IP, provide large interface area and tunable surface property that combined are conducive to strong adhesion towards metals forming tight coating protection against corrosion [71]. As shown in Fig. 10, it was demonstrated that PANI nanotubes synthesized at the Lm-L interface showed good anti-corrosion effect [72]. In this case, the use of decylphosphonic acid (DPA) as a dopant may provide further protection to the metal because phosphono groups can interact strongly with metal oxides (the passivating layer generated by coated PANI), and the released DPA ions contribute to the surface blocking by forming insoluble complex salts with iron.

Besides the polymeric blends, the combination of CPs with other

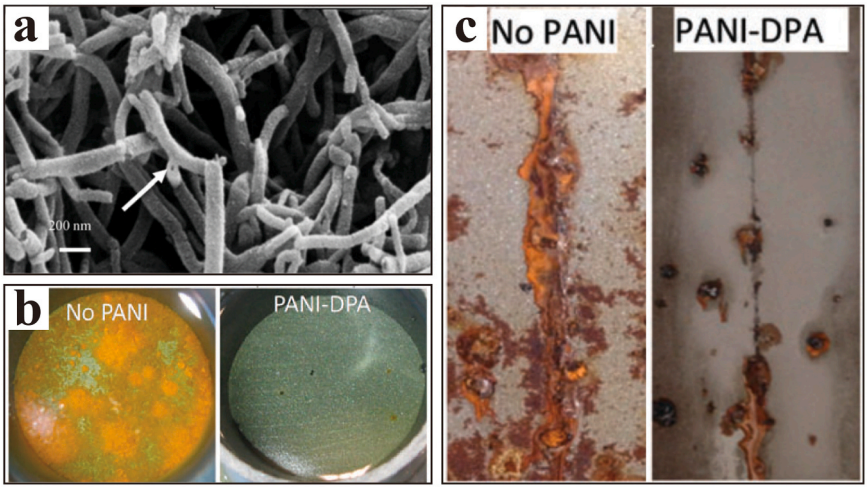

Fig. 10. (a) SEM image of PANI nanotubes obtained at Lm-L interface in which an arrow is used to indicate the cavity of nanotube. (b) Photos of the samples taken after a week immersion test in 3.5% NaCl solution. (c) Photos of the samples with a scratch taken after 20 days of salt spray test.
Reprinted with permission from Ref. [72]. Copyright 2016 Royal Society of Chemistry.

nanomaterials such as metal oxide nanoparticles and carbon nanomaterials (carbon black, CNT, graphene, *etc*.) also helps improve sustainability of anti-corrosion coating. Metal oxide nanoparticles have been widely used as reinforcement components to improve the corrosion resistance and mechanical properties of anti-corrosion coating. Graphene has been used in recent decades in combination with CPs due to its unique chemical inertness, excellent thermal stability and molecular impermeability. Although coatings based on IP or the NCPs fabricated from other methods have demonstrated good promise in corrosion resistance, the details of anti-corrosion mechanism and the correlated materials improvement still remain in debate and face some serious technical challenges, thus demanding more research in future.

3.4. Other applications

In addition to the three applications mentioned above, NCPs prepared by IP also have been used for other fields such as electro-responsive electrorheological [52], gas separation [24], contaminant adsorbent [61], photocatalysis [49], and electroactive tissue [58,59]. In most cases, these applications rely on NCPs-involved composites with another active material as well as tunable structures and interfaces.

When PANI was coated on the surface of poly(ionic liquid)s, the electro-responsive electrorheological effect can be enhanced, because the PANI shell can well limit the irreversible ion leakage of poly(ionic liquid)s microspheres and improve the particle polarizability. By increasing $FeCl_2$ concentration in $FeCl_3$ solution, IP reaction rate was reduced and the denser PPy nanofilm was prepared at Lm-L interface, which significantly improved its gas selectivity. The highest selectivity value was $O_2/N_2 = 17.2$ and permeability for O_2 was 40.2 barrer.

Recently, the use of CPs such as PANI or PPy as adsorbents for environmental remediation has shown great promise due to their excellent environmental stability, good redox reversibility, low cost, easy synthesis and treatment [73]. PPy/PANI composite films (Fig. 8) prepared at Vm-L interface show an excellent Cr(VI) adsorption capacity of 256.41 mg g^{-1}, much higher than that of PPy-based absorbents prepared by chemical and electrochemical polymerization [61]. Furthermore, PANI can also enhance the adsorption of organic dyes such as methylene blue and rhodamine B. PANI-modified MnO_2 composite nanorods via Lm-L IP showed higher photocatalytic efficiency than that of MnO_2 [49]. This is because the organic dyes can be well adsorbed on PANI/MnO_2 providing more contact sites than single component. The versatility, compatibility and biocompatibility of NCPs also make them attractive in electroactive tissue engineering. As shown in Fig. 11, unique hybridized materials was composed of NCPs and CNT at Vm-S interface. The resulting 3D scaffolds showed typical Young's modulus (20–50 kPa) of soft materials, as well as high electrical conductivity, which played an important role in electroactive cell growth.

4. Conclusions and prospective

As a promising method for NCPs synthesis, IP has attracted increasing interest in the research fields of CPs, taking advantages of the great tunability of interfaces, precursor materials (monomer, oxidant, *etc*.) and reaction conditions, which in turn provide NCPs prepared therefrom with diverse types regarding morphology and size. These unique features of NCPs and the associated IP synthetic methods provide enormous promise for the materials and related applications in supercapacitor, chemosensor and corrosion protection fields.

Upon reviewing the recent advancement in the fields, we identify three areas of research concerned improvement of IP and NCPs that deserve consideration and further endeavors. Firstly, most IP reactions reported are slow and limited in small reaction scale (e.g., limited by containers and interfaces), imposing potential challenge for their practical use as film devices and large-scale production. Secondly, the regulatory aspects and strategies are not consistent in relation to different interface systems. For the most studied Lm-L interfaces, although researchers have done systematic studies to adjust the nanostructures of NCPs through variable pathways, the precise control of NCPs into preferential dimensions and morphologies has yet been achieved, and more studies are still needed to realize a balance among monomer and its concentration, oxidant and reaction rate, solution-phase and the interface. For Lm-S interface, the selection of oxidants is extremely important for forming pure and uniform NCPs. Oxidants are either required not to be soluble in the liquid phase in order to limit the reaction at the interface, or stay absorbed stably on the solid substrate. For the Vm-S or Vm-L interface, the hygroscopicity of oxidant (solid phase) often hinders the polymerization reaction and damage the integrity of film morphology, while oxidant (in aqueous solution) interferes the water evaporation and pore generation especially at lower concentration. In addition, lower volatility of EDOT (vapor pressure of 0.278 mmHg at 24 °C) and some other monomers should also be seriously considered for their use in vapor-involved IP process. Thirdly, as described in Section 2, aniline has both high solubility and effumability, and remains the most commonly used monomer in IP to make high-ordered PANI nanostructures. In comparison, most of other CPs can only be synthesized from the monomers that are either poor in solubility

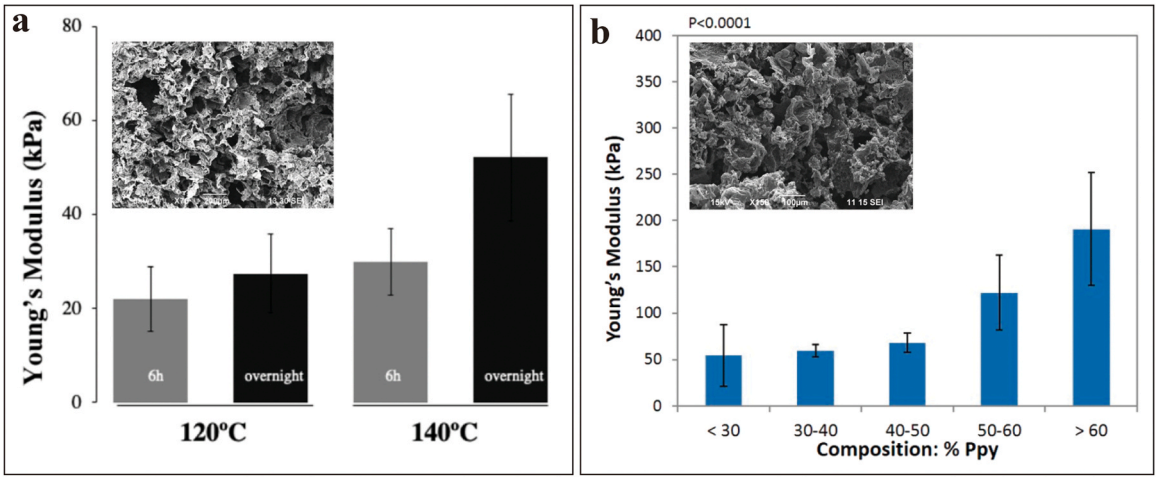

Fig. 11. (a) Young's Modulus of PEDOT/CNT scaffolds synthesized under different synthesis time and temperature at Vm-S interface. (inset: SEM images of PEDOT/CNT scaffolds). (b) Young's Modulus of PPy/CNT scaffolds related to the polymer composition. (inset: SEM images of PPy/CNT scaffolds).
(a) Reprinted with permission from Ref. [58]. Copyright 2020 American Chemical Society. (b) Reprinted with permission from Ref. [59]. Copyright 2018 American Chemical Society.

or effumability, thus hardly producing NCPs with highly ordered structure or morphology. Moreover, the redox property and structure planarity of monomer molecules also affect significantly the oxidation polymerization at the interface. Innovative design of new structures of pyrrole, thiophene, EDOT and other monomers may lead to better understanding of the IP process and more precise structural control of the synthesis of NCPs. Among them, our ongoing research has demonstrated the successful IP of 3-methoxythiophene by Iron(III) oxidant $Fe(OTs)_3$ in Lm-L (hexane-CH_3CN) interface system, which produces uniform nanofibers. In view of the unparalleled features of PEDOT in CPs, the analogs and derivatives of EDOT monomers should be taken more attention and deserve more research effort. In our previous work, monomers in these series have been synthesized and carried out for successful oxidative polymerization under conventional ways [74].

By blending with other nanomaterials (especially, metal oxides and carbon materials, patterned polymers, *etc*.), the hybrid composites of NCPs provide more options for property tuning and performance improvement when used in devices, such as organic electronics, flexible and wearable sensors, photo(electric)catalysis, energy transfer and storage units, gas separation membranes, drug delivery and among others. The research of IP could also be synergic to the study of surface-supported synthesis or other interfacial engineering like molecular self-assembly, with the aim to get better approaches to control and optimize IP and the structure of NCPs thus produced. As an evidence, Qin et al. [75] has established a controllable interfacial supramolecular polymerization method to achieve polymers of $(UPy\text{-}SH)_2$ (dimerization of ureidopyrimidinone (UPy) units forming two thiol end groups) with effective control of their properties. Moreover, our group has recently tried to fabricate 1D aggregates of EDOT unit-attached PTCDIs via supramolecular self-assembly for electrochemical research [15] and potential performance in fluorescence chemosensor application [76]. Ternary oligomers of stereoregular fused thiophenes like thineo[3,2-b] thiophene (TT) with EDOT have also been synthesized in our lab, and these molecules have much planar and long-range conjugation architecture along the parallel direction [77,78], which show great promise for IP (in combination with molecular self-assembly) to prepare highly structured NCPs.

Declaration of Competing Interest

The authors declare that they have no known competing financial interests or personal relationships that could have appeared to influence the work reported in this paper.

Acknowledgments

The financial support of the China Scholarship Council (No. 201808360327) was gratefully acknowledged.

References

[1] M.X. Wan, Conducting Polymers with Micro or Nanometer Structure, Tsinghua University Press, Beijing, 2008.
[2] T.H. Le, Y. Kim, H. Yoon, Electrical and electrochemical properties of conducting polymers, Polymers 9 (2017) 150.
[3] X.G. Guo, A. Facchetti, The journey of conducting polymers from discovery to application, Nat. Mater. 19 (2020) 922–928.
[4] S. Ghosh, T. Maiyalagan, R.N. Basu, Nanostructured conducting polymers for energy applications: towards a sustainable platform, Nanoscale 8 (2016) 6921–6947.
[5] B.T. Zhang, H. Liu, Y. Liu, Y. Teng, Application trends of nanofibers in analytical chemistry, TrAC Trends Anal. Chem. 131 (2020), 115992.
[6] W.W. Zhang, W.N. Zhang, Z.X. Xue, Y. Xue, N.N. Jian, K. Qu, H. Gu, S. Chen, J. K. Xu, Electrochromic poly(N-alkyl-3,4-dihydrothieno[3,4-b][1,4]oxazine)s via electrosynthesis from green microemulsions, Electrochim. Acta 278 (2018) 313–323.
[7] Y. Xue, S. Chen, J.R. Yu, B.R. Bunes, Z.X. Xue, J.K. Xu, B.Y. Lu, L. Zang, Nanostructured conducting polymers and their composites: synthesis methodologies, morphologies and applications, J. Mater. Chem. C 8 (2020) 10136–10159.
[8] J.X. Huang, R.B. Kaner, A general chemical route to polyaniline nanofibers, J. Am. Chem. Soc. 126 (2004) 851–855.
[9] A.R. Hopkins, D.D. Sawall, R.M. Villahermosa, R.A. Lipeles, Interfacial synthesis of electrically conducting polyaniline nanofiber composites, Thin Solid Films 469–470 (2004) 304–308.
[10] P. Dallas, D. Stamopoulos, N. Boukos, V. Tzitzios, D. Niarchos, D. Petridis, Characterization, magnetic and transport properties of polyaniline synthesized through interfacial polymerization, Polymer 48 (2007) 3162–3169.
[11] J.B. Li, Q.M. Jia, J.W. Zhu, M.S. Zheng, Interfacial polymerization of morphologically modified polyaniline: from hollow microspheres to nanowires, Polym. Int. 57 (2008) 337–341.
[12] Y.Z. Long, M.M. Li, C. Gu, M. Wan, J.L. Duvail, Z. Liu, Z. Fan, Recent advances in synthesis, physical properties and applications of conducting polymer nanotubes and nanofibers, Prog. Polym. Sci. 36 (2011) 1415–1442.
[13] L. Zang, Interfacial donor-acceptor engineering of nanofiber materials to achieve photoconductivity and applications, Acc. Chem. Res. 48 (2015) 2705–2714.
[14] S. Chen, P. Slattum, C.Y. Wang, L. Zang, Self-assembly of perylene imide molecules into 1D nanostructures: methods, morphologies, and applications, Chem. Rev. 115 (2015) 11967–11998.
[15] Z.X. Xue, S. Chen, Y. Xue, O.A. Watson, L. Zang, Electrochemical study of structure tunable perylene diimides and the nanofibers deposited on electrodes, Langmuir 35 (2019) 12009–12016.
[16] M.J.T. Raaijmakers, N.E. Benes, Current trends in interfacial polymerization chemistry, Prog. Polym. Sci. 63 (2016) 86–142.
[17] Y. Wu, J.X. Wang, B. Ou, S. Zhao, Z. Wang, Some important issues of the commercial production of 1-D nano-PANI, Polymers 11 (2019) 681.
[18] Y.Y. Song, J.B. Fan, S.T. Wang, Recent progress in interfacial polymerization, Mater. Chem. Front. 1 (2017) 1028–1040.
[19] S.X. Xing, H.W. Zheng, G.K. Zhao, Preparation of polyaniline nanofibers via a novel interfacial polymerization method, Synth. Met. 158 (2008) 59–63.
[20] J.X. Huang, R.B. Kaner, The intrinsic nanofibrillar morphology of polyaniline, Chem. Commun. (2006) 367–376.
[21] D.D. Jin, Y. Zhou, T. Li, S. Hu, Y.Y. Shen, Y.W. Zhang, Z.Y. Qin, Efficient construction and enhanced capacitive properties of interfacial polymerized polyaniline nanofibers with the assistance of isopropanol in aqueous phase, Electrochim. Acta 257 (2017) 311–320.
[22] C.Z. Yuan, L.R. Hou, L.F. Shen, X.G. Zhang, Facile water/ionic liquid/organic triphase interfacial synthesis of coral-like polyaniline toward high-performance electrochemical capacitors, J. Electrochem. Soc. 159 (2012) A1323–A1328.
[23] X.G. Li, J. Li, Q.K. Meng, M.R. Huang, Interfacial synthesis and widely controllable conductivity of polythiophene microparticles, J. Phys. Chem. B 113 (2009) 9718–9727.
[24] W.I. Son, J.M. Hong, B.S. Kim, Polypyrrole composite membrane with high permeability prepared by interfacial polymerization, Korean J. Chem. Eng. 22 (2005) 285–290.
[25] S.Y. An, T. Abdiryim, Y.J. Ding, I. Nurulla, A comparative study of the microemulsion and interfacial polymerization for polyindole, Mater. Lett. 62 (2008) 935–938.
[26] B. Gupta, D.S. Chauhan, R. Prakash, Controlled morphology of conducting polymers: formation of nanorods and microspheres of polyindole, Mater. Chem. Phys. 120 (2010) 625–630.
[27] W. Sangwan, N. Paradee, A. Sirivat, Polycarbazole by chemical oxidative interfacial polymerization: morphology and electrical conductivity based on synthesis conditions, Polym. Int. 65 (2016) 1232–1237.
[28] K. Su, N. Nuraje, L.Z. Zhang, I.W. Chu, R.M. Peetz, H. Matsui, N.L. Yang, Fast conductance switching in single-crystal organic nanoneedles prepared from an interfacial polymerization-crystallization of 3,4-ethylenedioxythiophene, Adv. Mater. 19 (2007) 669–672.
[29] N. Nuraje, K. Su, N.L. Yang, H. Matsui, Liquid/liquid interfacial polymerization to grow single crystalline nanoneedles of various conducting polymers, ACS Nano 2 (2008) 502–506.
[30] Y.J. He, One-dimensional polyaniline nanostructures synthesized by interfacial polymerization in a solids-stabilized emulsion, Appl. Surf. Sci. 252 (2006) 2115–2118.
[31] J. Stejskal, I. Sapurina, M. Trchová, E.N. Konyushenko, Oxidation of aniline: polyaniline granules, nanotubes, and oligoaniline microspheres, Macromolecules 41 (2008) 3530–3536.
[32] T. Li, Z.Y. Qin, B.L. Liang, F. Tian, J.Y. Zhao, N. Liu, M.F. Zhu, Morphology-dependent capacitive properties of three nanostructured polyanilines through interfacial polymerization in various acidic media, Electrochim. Acta 177 (2015) 343–351.
[33] H.Y. Ma, Y.Q. Luo, S.X. Yang, Y.W. Li, F. Cao, J. Gong, Synthesis of aligned polyaniline belts by interfacial control approach, J. Phys. Chem. C 115 (2011) 12048–12053.
[34] A. Elschner, S. Kirchmeyer, W. Lövenich, U. Merker, K. Reuter, PEDOT-Principles and Applications of an Intrinsically Conductive Polymer, CRC Press, New York, 2011.
[35] F.X. Zeng, Z.Y. Qin, B.L. Liang, T. Li, N. Liu, M.F. Zhu, Polyaniline nanostructures tuning with oxidants in interfacial polymerization system, Prog. Nat. Sci. Mater. Int. 25 (2015) 512–519.
[36] C. Su, G.C. Wang, F.R. Huang, X.W. Li, Effects of synthetic conditions on the structure and electrical properties of polyaniline nanofibers, J. Mater. Sci. 43 (2008) 197–202.
[37] R.Q. Li, Z. Chen, J.Q. Li, C.H. Zhang, Q. Guo, Effective synthesis to control the growth of polyaniline nanofibers by interfacial polymerization, Synth. Met. 171 (2013) 39–44.

[38] B. Rajender, S. Palaniappan, Organic solvent soluble methyltriphenylphosphonium peroxodisulfate: a novel oxidant for the synthesis of polyaniline and the thus prepared polyaniline in high performance supercapacitors, New J. Chem. 39 (2015) 5382–5388.
[39] J. Jang, J. Bae, E. Park, Selective fabrication of Poly(3,4-ethylenedioxythiophene) nanocapsules and mesocellular foams using surfactant-mediated interfacial polymerization, Adv. Mater. 18 (2006) 354–358.
[40] Y.J. He, Interfacial synthesis and characterization of polyaniline nanofibers, Mater. Sci. Eng. B 122 (2005) 76–79.
[41] D.D. Jin, Z.Y. Qin, Y.Y. Shen, T. Li, L. Ding, Y.Y. Chen, Y.W. Zhang, Enhancing the formation and capacitance properties of interfacial polymerized polyaniline nanofibers by introducing small alcohol molecules, J. Solid State Electrochem. 22 (2018) 1227–1236.
[42] J.Y. Zhao, Z.Y. Qin, T. Li, Z.Z. Li, Z. Zhou, M.F. Zhu, Influence of acetone on nanostructure and electrochemical properties of interfacial synthesized polyaniline nanofibers, Prog. Nat. Sci. Mater. Int. 25 (2015) 316–322.
[43] H. Albaris, G. Karuppasamy, Inspection of room temperature hydrogen sensing property of nanostructured polypyrrole/polyaniline hetero-junctions synthesized by one-pot interfacial polymerization, Mater. Chem. Phys. 250 (2020), 123153.
[44] U. Male, B.S. Singu, P. Srinivasan, Aqueous, interfacial, and electrochemical polymerization pathways of aniline with thiophene: nano size materials for supercapacitor, J. Appl. Polym. Sci. 132 (2015) 42013.
[45] N.A. Abdelwahab, A.M. Ghoneim, M.A. Abd El-Ghaffar, Characterization and electrical properties of poly(aniline-co-2,4-dimethoxyaniline) nanostructures prepared by interfacial polymerization, Int. J. Polym. Mater. Polym. Biomater. 62 (2013) 533–539.
[46] P. Liu, X. Wang, Y.J. Wang, Design of carbon black/polypyrrole composite hollow nanospheres and performance evaluation as electrode materials for supercapacitors, ACS Sustain. Chem. Eng. 2 (2014) 1795–1801.
[47] K.J. Li, D.F. Guo, J.M. Chen, Y. Kong, H.G. Xue, Oil-water interfacial synthesis of graphene-polyaniline-MnO2 hybrids using binary oxidant for high performance supercapacitor, Synth. Met. 209 (2015) 555–560.
[48] U. Bogdanovíc, V.V. Vodnik, S.P. Ahrenkiel, M. Stoiljkovíc, G. Ciríc-Marjanovíc, J. M. Nedeljkovíc, Interfacial synthesis and characterization of gold/polyaniline nanocomposites, Synth. Met. 195 (2014) 122–131.
[49] H. Xun, J.L. Zhang, Y. Chen, H.L. Lu, J.X. Zhuang, J.L. Li, Synthesis of polyaniline-modified MnO_2 composite nanorods and their photocatalytic application, Mater. Lett. 117 (2014) 21–23.
[50] J. Metsik, M. Timusk, A. Šutka, M. Mooste, K. Tammeveski, U. Mäeorg, In situ investigation of poly(3,4-ethylenedioxythiophene) film growth during liquid phase deposition polymerization, Thin Solid Films 653 (2018) 274–283.
[51] H.N. Gao, J.H. Zhang, F.Y. Liu, Z. Ao, S.D. Liu, S.J. Zhu, D. Han, B. Yang, Fabrication of polyaniline nanofiber arrays on poly(etheretherketone) to induce enhanced biocompatibility and controlled behaviours of mesenchymal stem cells, J. Mater. Chem. B 2 (2014) 7192–7200.
[52] C. Zheng, Y. Liu, Y.Z. Dong, F. He, X.P. Zhao, J.B. Yin, Low temperature interfacial polymerization and enhanced electro-responsive characteristic of poly(ionic liquid) s@polyaniline core-shell microspheres, Macromol. Rapid Commun. 40 (2018), 1800351.
[53] H. Goto, J. Jwa, K. Nakajima, A.H. Wang, Textile-surface interfacial asymmetric polymerization, J. Appl. Polym. Sci. 131 (2014) 41118.
[54] J.X. Li, Y.X. Ma, In-situ synthesis of transparent conductive PEDOT coating on PET foil by liquid phase depositional polymerization of EDOT, Synth. Met. 217 (2016) 185–188.
[55] J.X. Li, M.J. Zhang, J. Liu, Y.X. Ma, Effect of attached peroxyacid on liquid phase depositional polymerization of EDOT over PI film with adsorbed ferric chloride, Synth. Met. 198 (2014) 161–166.
[56] U. Male, E.J. Jo, J.Y. Park, D.S. Huh, Surface functionalization of honeycomb-patterned porous poly(ε-caprolactone) films by interfacial polymerization of aniline, Polymer 99 (2016) 623–632.
[57] Y.F. Diao, H.Z. Chen, Y. Lu, L.M. Santino, H.M. Wang, J.M. D'Arcy, Converting rust to PEDOT nanofibers for supercapacitors, ACS Appl. Energy Mater. 2 (2019) 3435–3444.
[58] A. Dominguez-Alfaro, N. Alegret, B. Arnaiz, J.M. González-Domínguez, A. Martin-Pacheco, U. Cossío, L. Porcarelli, S. Bosi, E. Vázquez, D. Mecerreyes, M. Prato, Tailored methodology based on vapor phase polymerization to manufacture PEDOT/CNT scaffolds for tissue engineering, ACS Biomater. Sci. Eng. 6 (2020) 1269–1278.
[59] N. Alegret, A. Dominguez-Alfaro, J.M. González-Domínguez, B. Arnaiz, U. Cossío, S. Bosi, E. Vázquez, P. Ramos-Cabrer, D. Mecerreyes, M. Prato, Three-dimensional conductive scaffolds as neural prostheses based on carbon nanotubes and polypyrrole, ACS Appl. Mater. Interfaces 10 (2018) 43904–43914.
[60] M. Fabretto, K. Zuber, C. Hall, P. Murphy, H.J. Griesser, The role of water in the synthesis and performance of vapour phase polymerised PEDOT electrochromic devices, J. Mater. Chem. 19 (2009) 7871–7878.
[61] V.D. Thao, B.L. Giang, T.V. Thu, Free-standing polypyrrole/polyaniline composite film fabricated by interfacial polymerization at the vapor/liquid interface for enhanced hexavalent chromium adsorption, RSC Adv. 9 (2019) 5445–5452.
[62] S. Bhadra, J.H. Lee, Synthesis of higher soluble nanostructured polyaniline by vapor-phase polymerization and determination of its crystal structure, J. Appl. Polym. Sci. 114 (2009) 331–340.
[63] J. Yan, S.H. Li, B.B. Lan, Y.C. Wu, P.S. Lee, Rational design of nanostructured electrode materials toward multifunctional supercapacitors, Adv. Funct. Mater. 30 (2020), 1902564.
[64] Y.C. Wong, B.C. Ang, A.S.M.A. Haseeb, A.A. Baharuddin, Y.H. Wong, Review-conducting polymers as chemiresistive gas sensing materials: a review, J. Electrochem. Soc. 167 (2020), 037503.
[65] X.B. Yan, Z.J. Han, Y. Yang, B.K. Tay, NO_2 gas sensing with polyaniline nanofibers synthesized by a facile aqueous/organic interfacial polymerization, Sens. Actuators B 123 (2007) 107–113.
[66] H. Wang, S. Nie, H. Li, R. Ali, J.N. Fu, H.J. Xiong, J. Li, Z.Q. Wu, W.-M. Lau, N. Mahmood, R.N. Jia, Y.F. Liu, X. Jia, 3D hollow quasi-graphite capsules/polyaniline hybrid with a high performance for room-temperature ammonia gas sensors, ACS Sens. 4 (2019) 2343–2350.
[67] S. Chen, N. Gao, B.R. Bunes, L. Zang, Tunable nanofibril heterojunctions for controlling interfacial charge transfer in chemiresistive gas sensors, J. Mater. Chem. C 7 (2019) 13709–13735.
[68] M.P. Jia, M. Rolandi, Soft and ion-conducting materials in bioelectronics: from conducting polymers to hydrogels, Adv. Healthc. Mater. 9 (2020), 1901372.
[69] D.W. Deberry, Modification of the electrochemical and corrosion behavior of stainless steels with an electroactive coating, J. Electrochem. Soc. 132 (1895) 1022–1026.
[70] A. Kausar, Performance of corrosion protective epoxy blend-based nanocomposite coatings: a review, Polym.-Plast. Technol. Mater. 59 (2020) 658–673.
[71] B. Yao, G.C. Wang, J.K. Ye, X.W. Li, Corrosion inhibition of carbon steel by polyaniline nanofibers, Mater. Lett. 62 (2008) 1775–1778.
[72] C. Oueiny, S. Berlioz, F.X. Perrin, Assembly of polyaniline nanotubes by interfacial polymerization for corrosion protection, Phys. Chem. Chem. Phys. 18 (2016) 3504–3509.
[73] H.N.M.E. Mahmud, A.K.O. Huq, R.B. Yahya, The removal of heavy metal ions from wastewater/aqueous solution using polypyrrole-based adsorbents: a review, RSC Adv. 6 (2016) 14778–14791.
[74] S. Chen, B.Y. Lu, X.M. Duan, J.K. Xu, Systematic study on chemical oxidative and solid-state polymerization of poly(3,4-ethylenedithiathiophene), J. Polym. Sci. Part A Polym. Chem. 50 (2012) 1967–1978.
[75] B. Qin, S. Zhang, Q. Song, Z.H. Huang, J.F. Xu, X. Zhang, Supramolecular interfacial polymerization: a controllable method of fabricating supramolecular polymeric materials, Angew. Chem. Int. Ed. 56 (2017) 7639–7643.
[76] S. Chen, Z.X. Xue, N. Gao, X.M. Yang, L. Zang, Perylene diimide-based fluorescent and colorimetric sensors for environmental detection, Sensors 20 (2020) 917.
[77] Y. Xue, Z.X. Xue, W.W. Zhang, W.N. Zhang, S. Chen, K.W. Lin, J.K. Xu, Effects on optoelectronic performances of EDOT end-capped oligomers and electrochromic polymers by varying thienothiophene cores, J. Electroanal. Chem. 834 (2019) 150–160.
[78] Z.X. Xue, S. Chen, N. Gao, Y. Xue, B.Y. Lu, O.A. Watson, L. Zang, J.K. Xu, Structural design and applications of stereoregular fused thiophenes and their oligomers and polymers, Polym. Rev. 60 (2020) 318–358.